# High Field Superconducting Solenoids Via High Temperature Superconductors

Justin Schwartz, *Fellow, IEEE*, Timothy Effio, Xiaotao Liu, Quang V. Le, Abdallah L. Mbaruku, Hans J. Schneider-Muntau, Tengming Shen, Honghai Song, Ulf P. Trociewitz, Xiaorong Wang, *Student Member, IEEE*, and Hubertus W. Weijers

***Abstract*—High-field superconducting solenoids have proven themselves to be of great value to scientific research in a number of fields, including chemistry, physics and biology. Present-day magnets take advantage of the high-field properties of $Nb_3Sn$, but the high-field limits of this conductor are nearly reached and so a new conductor and magnet technology is necessary for superconducting magnets beyond 25 T. Twenty years after the initial discovery of superconductivity at high temperatures in complex oxides, a number of high temperature superconductor (HTS) based conductors are available in sufficient lengths to develop high-field superconducting magnets. In this paper, present day HTS conductor and magnet technologies are discussed. HTS conductors have demonstrated the ability to carry very large critical current densities at magnetic fields of 45 T, and two insert coil demonstrations have surpassed the 25 T barrier. There are, however, many challenges to the implementation of HTS conductors in high-field magnets, including coil manufacturing, electromechanical behavior and quench protection. These issues are discussed and a view to the future is provided.**

***Index Terms*—High-temperature superconductors, nuclear magnetic resonance, superconducting magnets, superconducting materials, superconducting tapes, superconducting wires.**

## I. Introduction

HIGH field superconducting magnets play an important role in scientific research. Nineteen Nobel Prizes, including sixteen in physics and three in chemistry, have been awarded for scientific discoveries related to either the use or generation of high magnetic fields. Seven of these have been awarded in the past twenty years. Much of the importance of high magnetic fields relates to the fundamental behavior of charged particles and their orbits around magnetic field lines; as the magnetic field increases, the radius of the particle orbit decreases, thereby allowing investigations of phenomena on smaller length scales. Specific examples of the impact of high magnetic fields on research are found in condensed matter physics, materials science, biology, chemistry, physiology and psychology [1]–[5]. Furthermore, superconducting magnets have been an essential enabling technology for particle accelerators and colliders and play an essential role in fusion devices, including the International Thermonuclear Experimental Reactor [6], [7].

The development of high-field superconducting magnets is driven primarily by the development of high-field superconducting materials [8]. Early superconducting solenoids were limited by the properties of NbTi. More recently, progress in $Nb_3Sn$ conductors have driven the maximum magnetic field obtainable above 20 T. Recent examples of high-field $Nb_3Sn$ solenoids include the ultra wide-bore 900 MHz (21.1 T) Nuclear Magnetic Resonance (NMR) magnet at the National High Magnetic Field Laboratory (NHMFL) and the 950 MHz (22.3 T) NMR magnet from Bruker. These systems demonstrate that high-field solenoids follow the development of high-field conductors quickly. $Nb_3Sn$ conductors, and the magnets in which they result, are approaching their limit in high-field performance as dictated by the upper critical field $(H_{c2})$, so it is important to assess the future of high-field superconducting conductors and magnets.

In this paper, the importance of and potential for superconducting solenoids generating magnetic fields above 25 T with high temperature superconductors (HTS) are discussed. The first part of the paper provides a few specific examples of the impact of high magnetic fields on science. The preponderance of the paper then focuses on the technological opportunities of HTS conductors and the challenges that must be overcome if higher magnetic fields are to be generated. Particular emphasis is placed on the progress and issues of HTS conductors, including Bi-Sr-Ca-Cu-O wires and tapes, Y-Ba-Cu-O coated conductors and $MgB_2$ wires. A necessary-but-not-sufficient condition for the implementation of a new conductor is high engineering critical current density $(J_E)$, so the high-field electrical performance of HTS conductors are discussed with an emphasis on low temperature behavior in engineering forms. The potential for significant improvements in $J_E(B)$ is discussed and the essential relationships between conductor processing technologies, manufacturing scale-up issues, and magnet manufacturing are assessed.

High $J_E(B)$ HTS conductors pose engineering challenges for high performance, high-field, superconducting magnets. Very slow quench dynamics has important implications for quench detection and protection. The conductor failure modes due to quenching are not understood and the quench limits are not well defined. There are also relationships between conductor electromechanics, the fundamental limits on $J_E$ and conductor homogeneity which may also impact high-field magnet development. Furthermore, there is evidence that quench-induced conductor degradation and electromechanics may be directly coupled such that the mechanical state of the

Manuscript received December 31, 2007. This work was supported in part by the U.S. National Science Foundation through the National High Magnetic Field Laboratory, Air Force Office of Scientific Research, Office of Naval Research, National Institutes for Health, and U.S. Department of Energy.

The authors are with the National High Magnetic Field Laboratory, Florida State University, Tallahassee, FL 32310 USA (e-mail: schwartz@magnet.fsu.edu).

Color versions of one or more of the figures in this paper are available online at http://ieeexplore.ieee.org.

Digital Object Identifier 10.1109/TASC.2008.921363

conductor influences the quench limits, and that a protected quench may reduce the conductor strain tolerance. These issues and their underlying science are discussed. Thus, this paper addresses the essential question: *can a new, high-field, integrated conductor & magnet technology evolve?*

## II. Motivations for High-Field Solenoids

Recent advances in high magnetic field science have been propelled by the development of a series of new solenoid magnets at the NHMFL. These include the 60 T controlled pulse resistive magnet (1998), 45 T DC hybrid magnet (1999), 35 T DC resistive magnet (2003), 900 MHz NMR magnet (2004), 14.5 T ion cyclotron resonance magnet (2004) and the 90 T multi-shot pulsed magnet (2006) [9]–[13].

One example of the benefits of high magnetic fields is in the study of quadrupolar nuclei. In this case, there is a reduction in second order broadening with increasing field and an improvement in sensitivity that scales $\sim B^4$. So, for example, in a study of the $^{17}$O shift in methyl alpha-D-glucopyranoside (a sugar) [14], NMR studies at 830 MHz (19.6 T) show a nineteen-fold increase in sensitivity and an 84-fold increase in speed as compared to data obtained at 400 MHz (9.4 T). The signal is larger and the line width narrower. Furthermore, the small signals in the 830 MHz spectrum are spinning sidebands from the magic angle spinning, which are not resolvable at 400 MHz. Another example is found in the studies of $Al_2O_3 + B_2O_3$ [15]. In this case, not only does the resolution significantly improve with magnetic field, but only at 25 T does it become possible to resolve the four different states of Al in the molecule. Another example from solid state NMR comes from the determination of member protein structures [16]. Consider the amino acid sequences of two membrane proteins, one of which is very short (KdpF) and one which is lengthy (Rv1861). Both are from mycobacterium tuberculosis and are potential drug targets. While the structure of the small protein can be solved, the spectra of the larger protein are too overlapped and higher fields are required to resolve the signals that provide the structural restraints; at 30 T, spectra of the larger proteins would be nearly completely resolved.

These examples represent only a few of many that can be found in chemistry, biology, physics, materials science, engineering and psychology. More detailed examples are discussed at length in the report by the *Committee on Opportunities in High Magnetic Field Science* (COHMAG), a Commissioned National Research Council Study [17]. COHMAG investigated the science and engineering that may be enabled by the production of higher magnetic fields and set targets for future magnet technology. Amongst the magnets targeted is a 30 T, superconducting, high resolution NMR spectrometer. This technological goal is based in part on the demonstration of a 25.05 T insert coil using $Bi_2Sr_2CaCu_2O_{8+x}$ (Bi2212) conductor, successfully tested in 2003 [18]. This was the first time a magnetic field greater than 25 T was generated by a superconducting material. More recently, another insert coil tested at the NHMFL generated 26.8 T using $YBa_2C_3O_{7-y}$ (YBCO) conductor [19]. Although this insert is significantly smaller in ID, OD and height, the average current density in the coil is at least double that of any previous record-setting high-field HTS insert coil. While COHMAG defines the motivation for higher field magnets, these test coils illustrate the potential of emerging HTS conductor technologies.

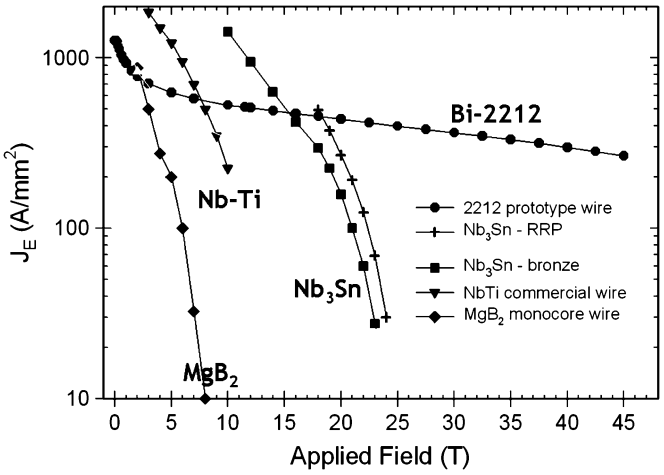


Fig. 1. $J_E(B, 4.2\ \mathrm{K})$ for low temperature superconductors and one HTS conductor, Bi2212. Although differences in the definition of $A_{cond}$ may skew some values, it is evident that the performance of $Nb_3Sn$ decreases rapidly above 20 T and that Bi2212 has significant potential at high fields [20].

## III. High-Field Superconducting Materials

The first metric that determines the applicability of a superconducting material is the transport critical current density as a function of magnetic field, $J_c(B)$. To compare magnet conductor options, the engineering critical current density, $J_E(B)$, is typically used because it factors in not only the performance of the superconductor itself, but the quantity of non-superconducting materials present. Thus, $J_E(B) = I_c(B)/A_{cond}$, where $I_c(B)$ is the transport critical current as a function of background magnetic field and $A_{cond}$ is the overall cross-section of the conductor. The conductor fill factor $f$ is defined as the fraction of the conductor area occupied by superconductor, $f = A_{SC}/A_{cond}$.

Fig. 1 plots typical $J_E(B, 4.2\ \mathrm{K})$ data for NbTi, $Nb_3Sn$, $MgB_2$ and Bi2212 wires [20]. It is important to note that this data is a "snapshot in time"; the conductors, and in particular $MgB_2$ and Bi2212, continue to improve. It is clearly seen that NbTi and $Nb_3Sn$ are severely limited above 12 T and 24 T, respectively. The poor high-field performance of $MgB_2$ wires is surprising. While $MgB_2$ has shown significant high-field behavior in thin films via proper doping [21], this has not been replicated in bulk or wire forms and thus $MgB_2$ cannot be considered a high-field conductor at present. If the thin-film results can be translated to wires, however, then the potential for $MgB_2$ as a low cost, high-field conductor is significant.

### A. High-Field Performance of HTS Conductors

While Fig. 1 plots the transport behavior of low temperature superconductors in comparison with Bi2212, Fig. 2 plots $J_E(B)$ to 45 T for Bi2212 conductors circa 2003–2004 and YBCO coated conductors circa 2005. This previously unpublished data is the only existing data at 45 T, however, and remains valuable as such. Data for two types of Bi2212 conductors are shown, round wires (RW, 0.8 mm diameter) and the wide (4 mm), thin

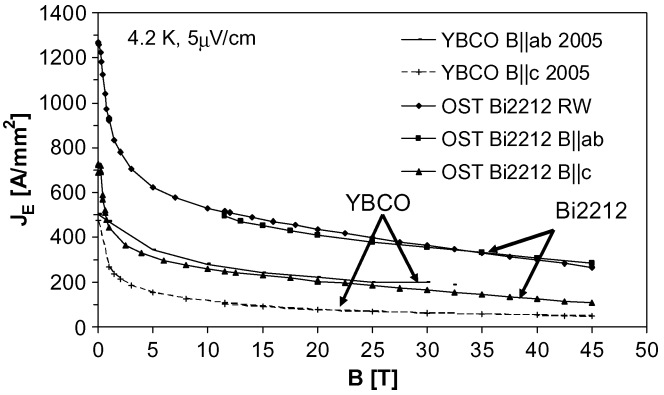


Fig. 2. $J_E(B, 4.2\ \mathrm{K})$ of Bi2212 wires and tapes and YBCO coated conductors in a background magnetic field up to 45 T. Although these conductors are now 2–4 years old and have been surpassed in performance by more recent versions, this is the only data available at such high fields and shows the weak dependence of $J_E$ on $B$ to fields well beyond those envisioned in superconducting magnets in the next decade. Note that the electric field criterion is 5 $\mu$V/cm. This is not applicable to the design of magnets, but is a limitation of the electrically noisy environment of the 45 T Hybrid magnet.

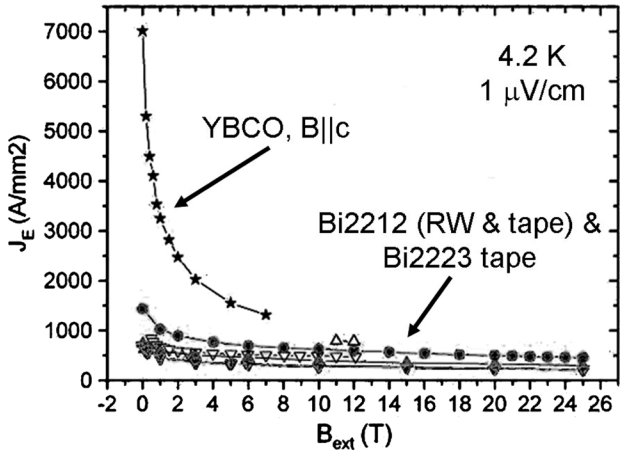


Fig. 3. $J_E(B, 4.2\ \mathrm{K})$ of circa 2007 Bi2212, Bi2223 and YBCO conductors in a magnetic field up to 25 T. In comparison with the data shown in Fig. 2 the quality of HTS conductors has improved significantly.

(0.2 mm) tapes used in the 25.05 T insert coil. Somewhat surprisingly, the Bi2212 round wire performs as well as the "good direction" $(B||ab)$ of the tape. This is not likely to be an intrinsic effect but rather due to filament-size effects, where the RW has a much higher filament count (>500 versus 19) and much smaller filaments than the tape conductor. There is a factor of four difference in the two orientations for the Bi2212 tape and a factor of three difference for the two orientations for the YBCO, illustrating the intrinsic electromagnetic anisotropy in these conductors.

More recent transport measurement results to 25 T on circa 2007 conductors are shown in Fig. 3, with cross-sectional images of the conductors shown in Figs. 4 and 5 [22]–[24]. In this case, the y-axis range is a factor of five greater than in Fig. 2. In Fig. 3, only data for the $B||c$ ("bad-direction") for YBCO is shown; the critical current for $B||ab$ is at least four times as high. Thus, YBCO $J_E(B)$ performance has increased by about a factor of five relative to the data in Fig. 2 and now surpasses that of Bi2212. These improvements illustrate the significant improvement in understanding YBCO developed from intense study during the past ten years. One of the most important issues

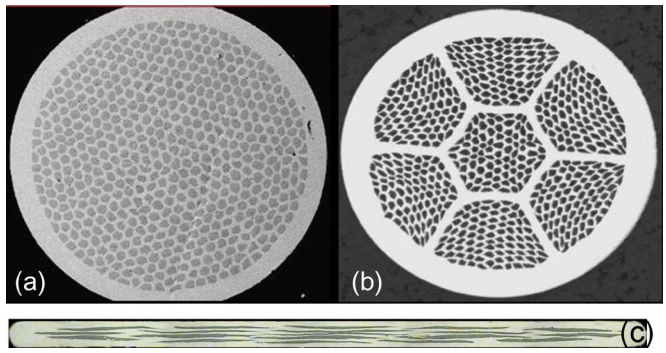


Fig. 4. Cross-sections of multifilamentary Bi2212 round wires and tape before heat treatment. Shown are (a) single and (b) double restacked round wires from two different U.S. manufacturers and the (c) tape conductor used in the 25.05 T insert.

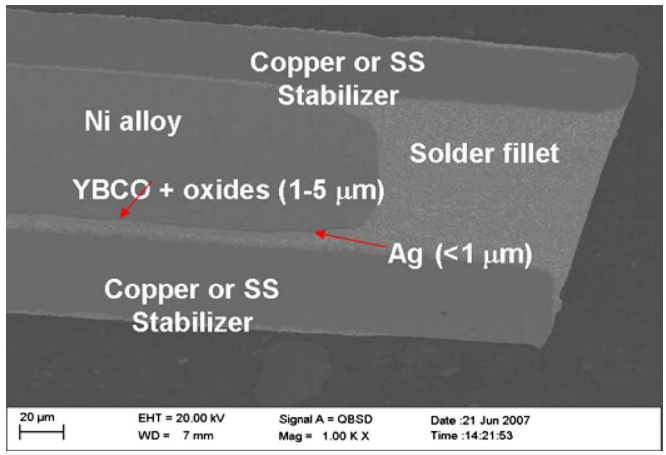


Fig. 5. Micrograph of the edge of a YBCO coated conductors from a U.S. manufacturer. Note that the superconductor fill factor, $f \sim 1\%$, which is typical of YBCO coated conductor from all manufacturers world-wide. Despite this, however, because the superconductor $J_c$ is very high, the $J_E$ is also very high.

to be resolved is that of the thickness dependence, in which the $J_c$ of the YBCO layer decreased significantly as the layer thickness increased. This is now understood as a combination of two factors, the through-thickness varying porosity (density) which is modeled effectively via Effective Medium Theory, and flux pinning [25]–[27]. As a result, $J_c$ (77 K, s.f.) ~4–5 MA/cm$^2$ is now obtained in thick YBCO layers. Future improvements in self-field $J_E$ are not likely to be driven by improvements in $J_c$, but rather in thicker YBCO layers and thinner packaging. As the ability to tailor flux-pinning defects continues to improve, the ability to design the conductor for the magnetic field required by the application is likely to evolve. Furthermore, because recent breakthroughs in magnetic flux pinning engineering affect both the magnetic field dependence of $J_c$ and electromagnetic anisotropy, the field dependence of the YBCO data in Fig. 2 is not likely to result in a universal curve for YBCO and present and future YBCO conductors are likely to behave somewhat differently. More details on YBCO conductor manufacturing can be found elsewhere [28].

Fig. 3 also shows improvement in the Bi2212 RW relative to Fig. 2; since the collection of the data in Fig. 3, Bi2212 RW has improved even further [29]–[31]. While improvements in Bi2212 wires are less dramatic than in YBCO, Bi2212 has never received the level of R&D that YBCO has received, and

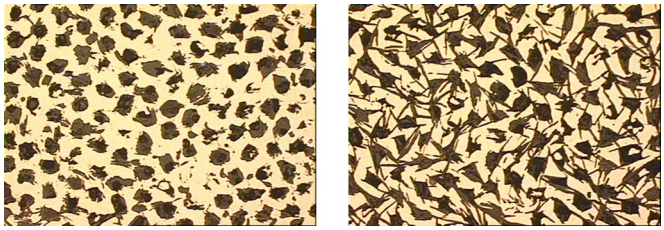

Fig. 6. Optical micrographs of Bi2212 wire before (left) and after (right) heat treatment, showing significant bridging between filaments after heat treatment. The conductor on the right has $J_E \sim 2$ kA/mm$^2$.

as a result a thorough understanding of Bi2212 has not yet developed. Significant improvements are anticipated in the near future as the research focus intensifies. For example, the post heat-treatment cross-sections of the highest $J_E$ conductors show microstructures that are dominated by interfilament bridging [30]–[32]. This is seen in Fig. 6, which shows optical micrographs before and after heat treatment. The heat treated wire has extensive interfilament bridging and very high $J_E$ ($\sim 2$ kA/mm$^2$ at 4.2 K, s.f.). Images of this type, which have been characteristic of Bi2212 from many manufacturers for over a decade, raise fundamental questions regarding where the current flows in Bi2212 multifilamentary conductors. Other significant unanswered questions include: what are the microscopic current limiting mechanisms in Bi2212 conductors? Why is round wire capable of high, isotropic $J_E$? As these questions are answered and Bi2212 is better understood, significant improvements in $J_E$ are expected.

### B. Implications for High-Field Superconducting Magnets

The data in Figs. 1–3, as well as similar progress by other HTS conductor manufacturers [32]–[34], illustrate three particularly important points. Firstly, the performance of HTS conductors continues to improve and further improvements are anticipated. Secondly, while Bi2212 and YBCO are demonstrated in insert coils to fields at or just above 25 T, conductor $J_E(B)$ is sufficient for magnets to at least 45 T. Thus, if the short-sample $J_E(B)$ performance is replicated in coils, electrical transport is not likely to be the performance-limiting factor. This is notably different from NbTi and $Nb_3Sn$ magnets. Lastly, from the $J_E(B)$ perspective, YBCO appears to be the best high-field conductor. Bi2212 remains of great interest, however, because it is the only round wire option beyond $Nb_3Sn$, and thus does not have to address issues related to anisotropic behavior that can strongly influence solenoid design [35], [36]. Furthermore, for high energy physics applications, round wires offer attractive options for cabling [37]. Lastly, one notices in Fig. 3 that Bi2223 has properties that are comparable to Bi2212. Bi2223, however, is not considered further because it is unlikely to have a low temperature, high-field niche. If tape conductor is acceptable, then Bi2223 is not competitive with YBCO. Thus, YBCO and Bi2212 remain the primary options for high-field magnets.

## IV. Engineering Issues for High-Field HTS Magnets

There remain significant engineering issues that must be addressed before high-field HTS magnets become commonplace. The first is conductor availability in long lengths and sufficient quantities. This is not an intrinsic engineering problem but rather a question of commercial scale-up requiring sufficient market pull. HTS development has been dictated by conductor push, but the investment required for scale-up requires a market for the final product. The push for high-field solenoids [17] and the quest for a high energy collider beyond the Large Hadron Collider (LHC) may provide the necessary pull in the near term. It is important to note that it was the market pull of the Tevatron, followed by the MRI industry and the LHC, that provided the market pull for NbTi. The conductor development programs of the high energy physics community, and more recently the LARP program, have helped provide market pull for $Nb_3Sn$ [38].

### A. Conductor Processing and Magnet Manufacturing

As increasing quantities of HTS conductors become available, it is important to evaluate magnet manufacturing options. Traditionally there are two approaches: React-&-Wind (R&W) and Wind-&-React (W&R). R&W has the advantage of separating the conductor processing from the magnet manufacturing. Thus, materials to be incorporated into the magnet are not exposed to the conductor heat treatment. With R&W, however, the conductor experiences significant bending strain due to winding into the magnet form. For small-bore, high-field magnets, the bending strain can be significant and strain management is an important and often performance-limiting issue [39], [40]. Thus, R&W is limited to magnets that are not strain limited. NbTi magnets, while not technically R&W because there is not a "reaction" step, are wound into magnets after conductor manufacture is complete and the bending strains associated with winding are accommodated in the design similar to R&W systems. Alternatively, with W&R manufacturing the magnet is formed in its final geometry, including the incorporation of turn-to-turn insulation and co-wound reinforcement, before final heat treatment. The bending strain is released during heat treatment because the superconducting phase is formed after packaging and in its final geometry. This approach is typically used for $Nb_3Sn$ magnets because of its strain sensitivity. For $Nb_3Sn$, insulation and reinforcement must be compatible with a heat treatment at $\sim 700$°C in an inert atmosphere.

Decisions regarding coil manufacturing are strongly influenced by conductor processing requirements. YBCO conductors are manufactured via thin film processing technologies that are incompatible with W&R manufacturing. Thus, all YBCO magnets will be R&W and magnet design must account for bending strain. The electromechanical behavior of YBCO is discussed later.

Bi2212 processing is significantly more complicated than YBCO and $Nb_3Sn$ and Bi2212 coil manufacturing remains a significant challenge [29], [41]–[43]. Bi2212 conductors are manufactured via a conventional powder-in-tube approach with Ag and Ag-alloy tubes. The approach is conceptually similar to multifilamentary NbTi and $Nb_3Sn$, with wire drawing and restacking to produce the multifilamentary cross-sections seen in Fig. 4. Like $Nb_3Sn$, Bi2212 requires a high temperature heat treatment after final deformation to produce high $J_E(B)$. Unlike $Nb_3Sn$, however, the Bi2212 heat treatment must be performed in oxygen (typically 100%) and the peak temperature ($T_{max}$) must be controlled within a few °C. A typical heat treatment schedule is shown in Fig. 7 where $T_{max} \sim 890$°C.

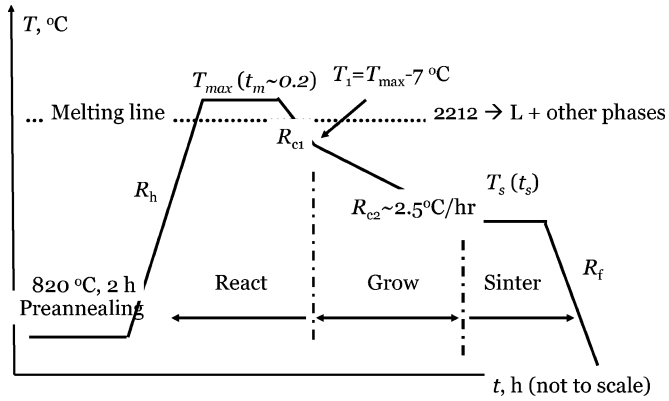


Fig. 7. Conventional $T - t$ heat treatment profile for Bi2212 conductors.

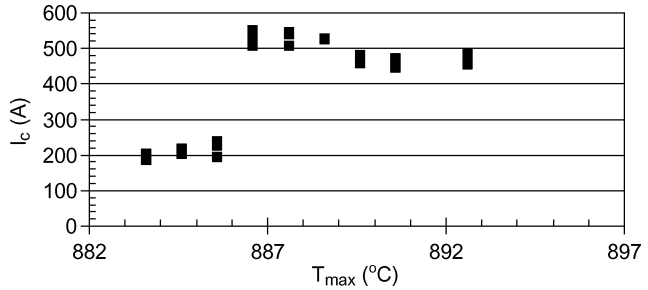


Fig. 8. Typical $I_c$ versus $T_{max}$ for Bi2212 conductors, illustrating the importance of peritectic melting.

Control of $T_{max}$ is vital because it must be above the peritectic melting point of Bi2212 such that significant liquid phase is formed from which the high $J_c$ Bi2212 grows during resolidification. If $T_{max}$ is too low, insufficient melting occurs and performance is poor. If $T_{max}$ is too high, a number of problems can result in reduced $J_E$, including phase separation and increased leakage of the Bi2212 through the sheath. Typical $I_c(T_{max})$ is seen in Fig. 8, showing that $I_c$ increases by 275% as $T_{max}$ increases from 886°C to 887°C, but decreases by ~20% from 888°C to 890°C.

Successful Bi2212 insert coils have been manufactured using both R&W and W&R manufacturing [35], [44]–[47]. Due to the complexity of the Bi2212 heat treatment, from a manufacturing perspective R&W is preferred. As discussed later, however, Bi2212 conductors are strain sensitive and the bending strain associated with R&W is unacceptably limiting for high-field magnets. W&R manufacturing has proven to be a significant challenge for Bi2212 magnets, and as the size of coils has increased, coil performance relative to short-sample conductor performance has decreased. This is likely to be related to inhomogeneous temperature and/or oxygen distributions during heat treatment. If the temperature is inhomogeneous, then either parts of the coil do not reach $T_{max}$ or other parts may either be overheated or held at $T_{max}$ for too long. Recent coil studies indicate that reducing $T_{max}$ and increasing the time at $T_{max}$, $t_m$, may offer improvement. If the oxygen distribution in the coil is inhomogeneous during heat treatment, inhomogeneous melting may result because the melt temperature decreases as $pO_2$ decreases [48], so oxygen-deficient sections of the coil may over-melt, or undesirable phase assemblages in regions of the magnet with insufficient oxygen during resolidification may result. Thus, obtaining a heat treatment that is uniform

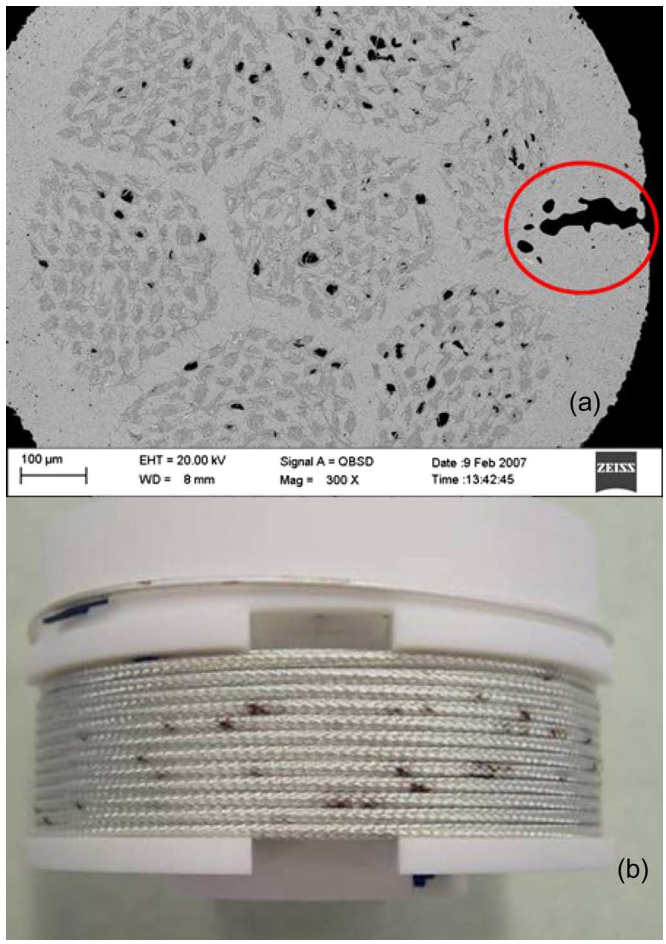


Fig. 9. (a) Cross-sectional SEM micrograph from a Bi2212 wire removed from a small test coil, showing the path of core leakage through the Ag and AgX sheaths, and (b), a typical leaky Bi2212 test coil on a macor coil former. Note that coils such as these typically carry ~60% of the current predicted by short-sample $I_c$ behavior [50].

in temperature and $pO_2$, such that the innermost sections of the coil are properly heat treated without over-processing the outermost regions, remains a significant challenge. Furthermore, because oxygen is required for Bi2212 processing, the options for insulation, coil former and reinforcement are limited. At best, current insulation options are undesirably thick, reducing the overall coil current density. At worst, the insulation enhances conductor leakage and interacts with the oxides that escape the wire [49]. This problem has plagued W&R Bi2212 conductors and coils for over fifteen years. Illustrations of leakage are shown in Fig. 9; (a) illustrates the path of molten oxide through the Ag sheath to the conductor edge and (b) shows a small W&R coil with a number of leakage spots randomly arrayed on the coil surface. A recent change from macor to inconel may significantly reduce leakage, however, and the complex chemistry of Ag, molten Bi2212, insulation and the coil former in oxygen is an important topic of Bi2212 R&D. Fig. 10 shows $I_c(B)$ results for two coils like that shown in Fig. 9, illustrating that progress in minimizing coil leakage is being made but that the effects of leakage are significant [50].

An alternative approach to Bi2212 coil manufacturing has been proposed that attempts to avoid the pitfalls of both R&W and W&R manufacturing. This approach, known as

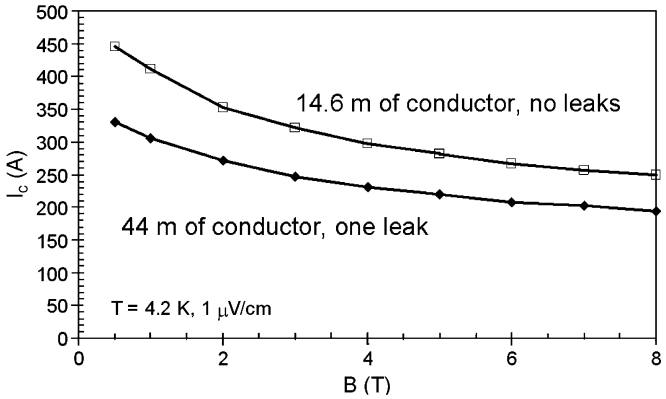


Fig. 10. $I_c(B)$ for two test coils like that shown in Fig. 9(b). Note that the coil with less conductor and no leaks has ∼25% higher performance than the large coil with one leak [50].

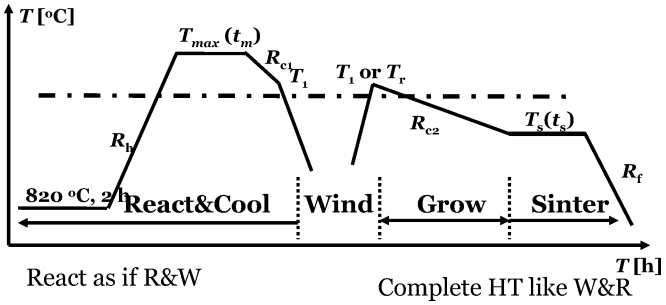


Fig. 11. Typical split heat treatment used in the React-Wind-Sinter approach to Bi2212 coil manufacturing. Note that $T_{max}$ remains the same as in conventional processing.

"React-Wind-Sinter" (RWS) and illustrated in Fig. 11, splits the heat treatment into two separate steps [30], [31], [51], [52]. The "react" step is performed on a large heat treatment mandrel as if R&W were being used. Thus, the key partial-melt step is performed with the conductor not in a tightly wound geometry and oxygen and temperature uniformity are less challenging. The conductor is then cooled to room temperature, the coil wound into final form (like W&R), and the heat treatment completed primarily within the Bi2212 solid state. Fig. 12 shows $I_c(B)$ data for Bi2212 round wires heat treated with the process shown in Fig. 11 and the conventional process shown in Fig. 7 with identical $T_{max}$. The RWS heat treatment results in a 30% increase in performance. Results like those in Fig. 12 and other studies [30], [31], [51], [52] show that RWS may not only avoid many of the problems with R&W and W&R Bi2212 manufacturing but also significantly improve Bi2212 performance. These results illustrate that Bi2212 processing and magnet manufacturing remain far from optimized.

### *B. Electromechanical Behavior*

High-field magnets intrinsically have large Lorentz forces $(F_L)$ because $F_L \sim JBR$, where $J$ is the overall current density, $B$ is the magnetic field generated and $R$ is a typical scale-length for the magnet size. Since typically $B \sim J$ (and in general, high $J$ is desired for reduced cost), $F_L$ scales with $B^2$. Thus, stress and strain management are important issues in the design of high-field conductors and magnets [39], [40]. It is also important to note that although high-field solenoids have very large forces, the simplicity of the geometry relative

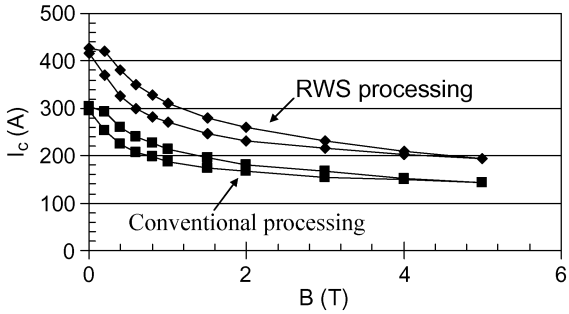


Fig. 12. $I_c$ versus magnetic field for RWS (upper curve) and conventional heat treatment (lower curve) Bi2212 round wires. RWS processing results in ∼30% improvement in conductor performance [30], [31], [52].

to other magnet applications (e.g. dipole magnets) simplifies the mechanics. Thus, while solenoid design is primarily concerned with mitigating the effects of hoop tension, other magnet geometries also must be concerned with bending modes and compression. All superconducting magnets must consider differences in thermal expansion between the superconductor and other materials present in the magnet. Furthermore, as discussed previously, the conductor electromechanical behavior influences magnet manufacturing decisions.

In the case of YBCO, magnets will be constructed using R&W manufacturing, so magnet design must consider the bending strain associated with winding, thermal strain and Lorentz forces. The conductor architecture, with a very thin YBCO layer sandwiched by thick metallic layers, implies that the bending strain in the YBCO layer may be relatively small, but within the metallic layers it can be significant. One could conceivably design an asymmetric conductor such that the YBCO layer has significant pre-compression from winding, though this may overly strain the stabilizer or impact other design issues, such as quench protection. A number of reports show that, to first order, the electromechanical behavior of YBCO coated conductors are dominated by the Ni-alloy substrates (Ni-W and Hastelloy) [53]–[58]. As a result, conductor strength and strain tolerance can be a conductor design variable, although considerations that determine conductor $J_E$ are likely to dominate the substrate selection. In general, YBCO coated conductors, and in particular those with Hastelloy substrates, are strong and sufficiently strain tolerant for high-field magnet applications. For example, the 26.8 T insert coil was not strain or stress limited. Fig. 13 shows the stress-strain and $I_c$-strain behavior of a typical YBCO coated conductor; similar data for other architectural variants are found in the literature. Interestingly, data from the most recent conductors has shown a reversible effect not seen in Fig. 13 nor in earlier work of most authors [57], [58]. This difference is attributed to improvements in the microstructure of the YBCO layer that eliminated the multiplicity of current paths that likely existed in earlier conductors. For magnets other than solenoids the dominant mechanical limits may be bending, compression, or tension normal to the conductor face, and issues related to interfacial shear and debonding may become important considerations. In these situations, the specifics of the conductor architectures and their manufacturing are likely to play more significant roles.

For Bi2212 conductors the electromechanical behavior is more complicated and is influenced by the behavior of the

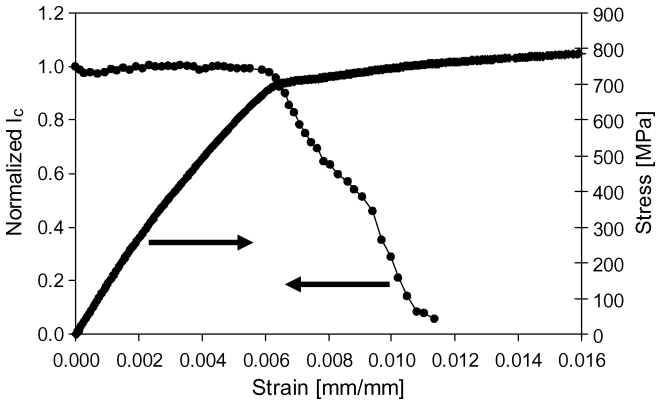


Fig. 13. Typical $I_c(\varepsilon)$ and $\sigma - \varepsilon$ behavior for YBCO coated conductor [55].

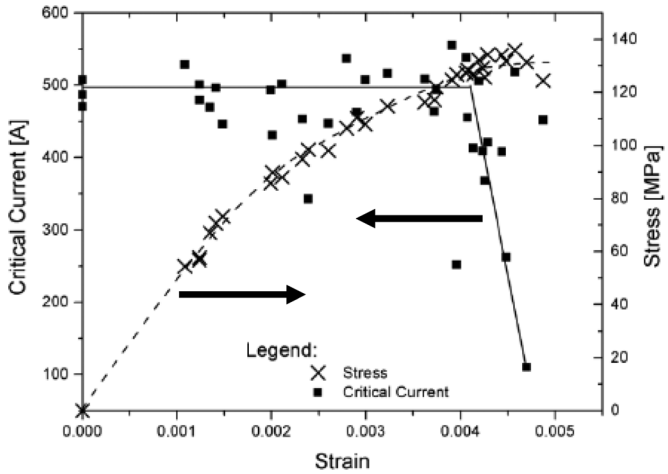


Fig. 14. Typical $I_c(\varepsilon)$ and $\sigma - \varepsilon$ behavior for Bi2212 tape conductor [62].

Ag and Ag-alloy sheaths, the microstructure of the Bi2212 filaments and differential thermal contraction [59]–[63]. In general, because of the relative lack of strength and stiffness of Ag and Ag alloys, Bi2212 conductors are highly strain sensitive. As a result, it is unlikely that future Bi2212 high-field solenoids will be R&W. Note that the 25.05 T insert used R&W manufacturing, but in that case the Bi2212 conductor was thin tape which experiences less bending strain than round wires. The advantages of round wire, e.g. isotropic electromagnetic behavior, increased $J_E$, smaller filaments, lower insulation volume fraction, etc., are pushing the development of round wires rather than tapes, so Bi2212 coil development is focused on round wire technologies. It is also difficult to find advantages of Bi2212 tape over YBCO tape, so if Bi2212 is to be competitive, it will be as a round wire.

Fig. 14 plots typical stress-strain and $I_c$-strain data for Bi2212 tape conductors [62]. The scatter in the $I_c$-strain data is indicative of the conductor inhomogeneity, which has more recently been quantified using Weibull statistics [63]. The Weibull analysis shows that there are clear differences between the mechanical and electrical failure within Bi2212 tapes, which is indicative of a strong role for microstructural inhomogeneities within the Bi2212 filaments. As seen in Fig. 15, the Weibull analysis shows significant scatter in the electromechanical performance of the tapes. While the scatter illustrates the conductor inhomogeneity, the relatively high reliabilities found in strained conductors are significant. For example, consider the data for $\varepsilon =$

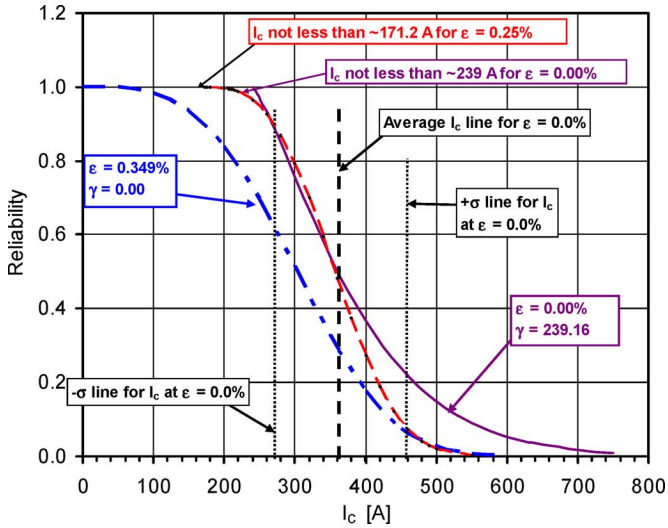


Fig. 15. Weibull reliability distributions for critical current at fixed levels of strain in Bi2212 tape conductor [63]. The conductor had an average $I_c = 378$ A and a critical strain of 0.349%.

$0.349\%$, which is the roughly the critical strain ($\varepsilon_c$). The reliability at $I = 378$ A (the unstrained batch-average $I_c$) is ~0.30, indicating that ~30% of the conductor maintains $I_c = 378$ A at this strain. If one considers $I \sim 190$ A (50% of the original batch average), the reliability is over 80%. Furthermore, it is interesting to consider the trends in the $\varepsilon = 0.25\%$ curve. For reliabilities above 0.50, the curve deviates only slightly from the zero-strain data, indicating that there is no effect on transport; i.e., all of the Bi2212 that carries current is insensitive to this level of strain. At high current (reliability ~0.10), the $\varepsilon = 0.25\%$ and $\varepsilon = 0.349\%$ curves converge, indicating that there is portion of current-carrying Bi2212 that is particularly strain-tolerant. *These are clear indicators that there is significant potential to improve the electromechanical behavior of Bi2212 through improved Bi2212 microstructure*. Thus, as $J_E$ increases through improved understanding of Bi2212, improved electromechanical performance is also anticipated. Not surprisingly, recent data indicates that the highest performing Bi2212 round wires also have significantly higher $\varepsilon_c$ (~0.6%) than the Bi2212 tapes described in the Weibull study. It will be interesting to see if the improved $\varepsilon_c$ corresponds to more homogeneous behavior as defined by statistical analysis.

### C. Quench Protection

Like the Lorentz force, the stored energy in a magnet scales with $B^2$ and the size of the magnet. Thus, high-field solenoids are high energy and high energy density systems and effective quench protection is essential for safe operation, particularly when system cost on the order of $10 M is anticipated. In general, quench protection in HTS magnets is qualitatively similar to that in low temperature superconductor (LTS) magnets, requiring detection of a disturbance or normal zone, a determination if the disturbance is unstable, and the triggering of the protection systems to prevent damage to the magnet. The basic physics and general mathematical formulations that describe quench phenomena in HTS magnets are the same as that for

LTS magnets, but because of significant differences in the material properties, quench protection in HTS systems may prove to be quite different and more challenging than in LTS systems.

The quench behavior of Bi2212 and YBCO short samples and small coils has been reported [64]–[81]. While the results vary with the specifics of the experimental approach and conductor architecture, a few general themes are consistently found. Firstly, HTS conductors have large energy margin and high heat loads *may* be tolerable. This is likely to be more important for high energy physics and/or fusion magnet applications. Secondly, normal zone propagation is very slow; typically two orders of magnitude slower than $Nb_3Sn$. Lastly, HTS conductors can be damaged by quenching and the failure limits, which in turn dictate the requirements of the protection system, are not yet quantified in detail. The failure limits are likely to be dependent on the conductor architecture and thus significant differences between Bi2212 and YBCO may be seen. In fact, there may be significant differences between YBCO manufacturers because of differences in the ways the conductors are packaged.

A number of studies have investigated quenching in YBCO conductors and coils [65]–[71], [74], [75], [79]–[81]. The number of potentially important variables is significant and makes comparisons of results difficult. One experimental variable is the mechanism by which quenching is induced. In one approach, quenches are initiated by taking advantage of inhomogeneities in the conductor $I_c$. The transport current is fixed such that it is below the end-to-end $I_c$ but above that of local "weak-spots". Joule heating causes weak-spots to become hot-spots. An alternative approach involves pulsing an external heater that is mounted to the conductor. In this way, the conductor transport current is a freely selected variable, but the total energy into the conductor is more difficult to determine because some of the energy is dissipated in the material (epoxy) that attaches the heater to the conductor and in the surrounding atmosphere. The latter approach has been used to study architectural variations in YBCO coated conductors, the performance of Bi2212 tapes and wires, and small coils of each material. Typically, these experiments result in data like that seen in Figs. 16 and 17, which show the voltage and temperature versus time at different locations within a conductor [72]. This data is used to determine if the conductor or coil quenched or recovered, and in the case of a quench, the normal zone propagation velocity. The long timescales on the x-axes of these figures are indicative of the slow quench dynamics in HTS materials.

Fig. 18 shows self-field normal zone propagation results for three YBCO coated conductor architectures like those shown in Fig. 5. In this experiment, the conductors are identical except for variations in the outer metal layers. Here, "Cu-Cu" refers to a conductor with Cu on each side, "Cu-SS" refers to a conductor with Cu on one side and stainless steel on the other, and "SS-SS" refers to a conductor with stainless steel on both sides. It is interesting to note that there is little difference between the "Cu-Cu" and the "Cu-SS", indicating that once a certain Cu thickness is present, additional Cu does not affect propagation. There is a significant increase in the propagation velocity in the absence of Cu ("SS-SS" conductor). Thus, if quench propagation is a limiting condition for protection, there may be advantages to *reducing* the amount of Cu present in favor of a SS or another stabilizer. More generally, conductor optimization may now include a range of options for stabilizer that consider both the requirements for quench protection and mechanical strength.

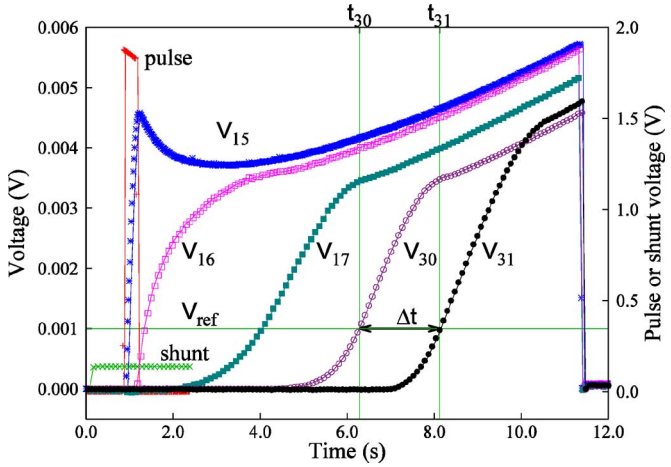


Fig. 16. Voltage versus time during a typical quench propagation experiment on an HTS conductor. V15, V16, V17, V30 and V31 refer to voltage taps along the length of the conductor. $\Delta t$ refers to the propagation time of the normal zone from one voltage tap set to the next; thus the propagation velocity is the distance between the taps divided by $\Delta t$.

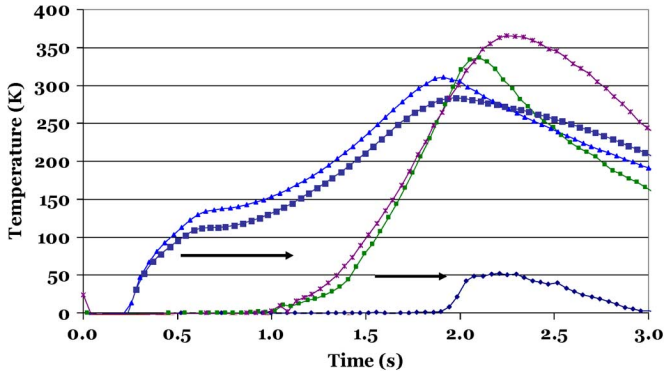


Fig. 17. Temperature-time data corresponding to the voltage-time data shown in Fig. 16. The different curves represent different locations along the length of the conductor; the arrows illustrate normal zone propagation.

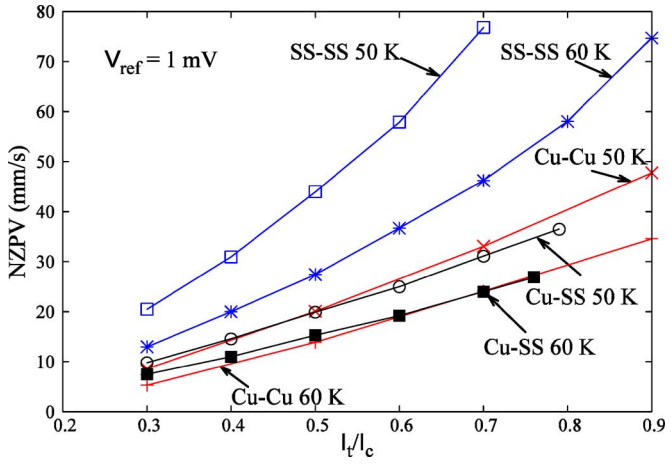


Fig. 18. Normal zone propagation velocity versus $I/I_c$ for YBCO coated conductors of various architectures at two different temperatures. The data is obtained from voltage-time data similar to that seen in Fig. 16.

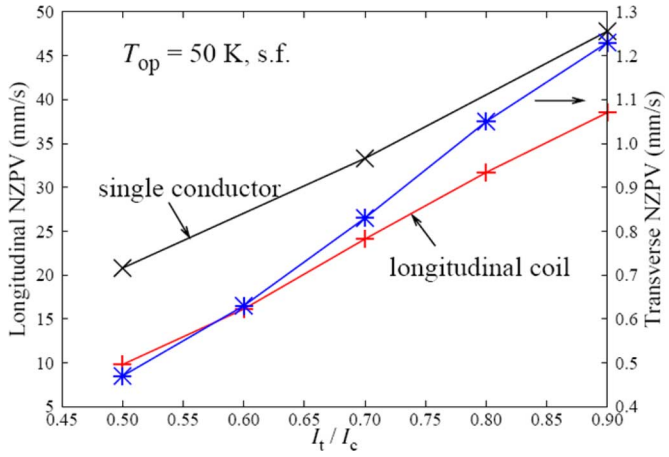


Fig. 19. Normal zone propagation in a YBCO coated conductor and a pancake coil made of the same conductor. Longitudinal propagation in the coil is about half that of the single conductor. Transverse propagation is a factor of ~20–35 slower.

Recent coil measurements that under certain circumstances quench propagation may be faster than previously measured and that there may be two "stages" to such propagation, including an initial stage with slow propagation, followed by a second stage with much faster propagation. This remains unconfirmed, however, and further study is required.

It is also important to consider the temperature and atmosphere dependences of the propagation velocity. The data shown in Fig. 18 are at 50 K and 60 K in vacuum, and the velocity increases as temperature decreases. Recent measurements at 4.2 K in liquid helium show roughly a factor of two increase in velocity relative to the 50 K results. Thus, for example, at $I \sim 50\%I_c$ in a SS-SS conductor, the propagation velocity reaches ~90 mm/s. This is the fastest propagation reported in any HTS conductor, but remains significantly slower than $Nb_3Sn$ and NbTi conductors. Based solely on temperature effects, one would expect a larger increase; the effectiveness of helium cooling at the surface, as compared to the experiments in vacuum, slows the propagation.

It is also pertinent to consider the quench propagation behavior in a coil as opposed to short samples to determine if short sample measurements are relevant to coil design. Fig. 19 compares the propagation results for the Cu-Cu conductor shown in Fig. 18 with results from a similar self-field experiment on a pancake coil made of the same conductor. The propagation in the coil is slower than the single conductor. One may have expected the opposite due to the effects of self-field, but instead the greater thermal mass of the coil dominates the behavior. It is also interesting to note that transverse propagation in the coil is ~20X slower than longitudinal propagation. Large differences between longitudinal and transverse propagation velocity are also reported in [80].

There is recent data on the quench behavior of Bi2212 tapes and round wires in liquid helium using an otherwise similar experimental approach as the YBCO results [76]–[78]. In this case, propagation velocities ~20–30 mm/s are found in tapes and ~60–80 mm/s in round wires. The difference is believed to be primarily related to the $J_E$ differences in the two conductors; as $J_E$ increases, so does the propagation velocity.

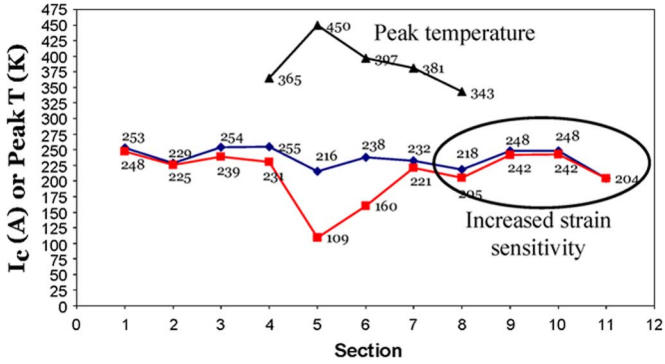


Fig. 20. Evidence of degradation of a YBCO coated conductor due to a quench. The upper curve is the hot-spot temperature versus location in the conductor during the quench experiment. The lower two curves show $I_c$ versus location before and after the quench. Degraded performance correlates directly with the hot-spot temperature. The section of conductor indicated by the oval, which did not show a reduction in $I_c$, was later found to have a reduced critical strain [82].

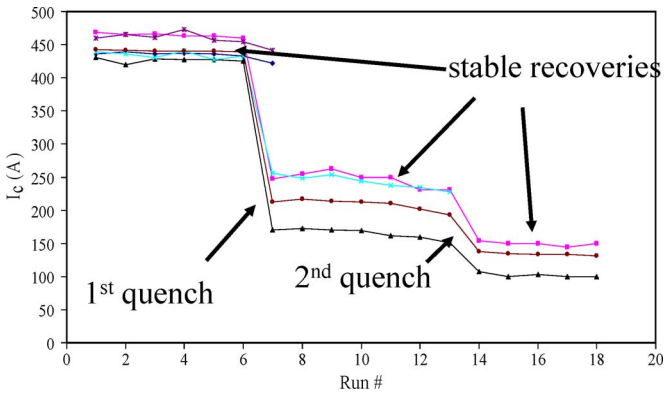


Fig. 21. Quench degradation in Bi2212 tape conductors due to quenching. Each curve refers to a different location within one conductor. It is seen that heat pulses that do not induce quenching also do not induce degradation. Quenches that do induce quenching, however, also degrade most of the conductor.

In any superconducting magnet, the protection system is designed to prevent superconductor degradation due to a quench, and experiments on YBCO and Bi2212 conductors and coils have that degradation is possible. A typical example for YBCO is seen in Fig. 20 [82]. Here, the upper curve shows the hot-spot temperature during the quench and the lower two curves show $I_c$ before (upper) and after (lower) the quench. From this and other similar experiments, it appears that the safe operational limit during the quench of a YBCO coil can be either a hot-spot temperature limit, a peak temperature gradient limit, or a $dT/dt$ limit (thermal shock). It is also important to note that subsequent electromechanical measurements on a section of this conductor that experienced no reduction in $I_c$ due to the quench [the section within the oval on Fig. 20)] did show a significant reduction in $\varepsilon_c$ [82]. This indicates that the quench protection limits may not be derived solely from reduced electrical performance, but that instead a new metric that accounts for this behavior will be required. This requires further study.

A systematic study of quench degradation in Bi2212 tapes and wires indicates that degradation in these conductors correlates with conductor performance. Fig. 21 plots $I_c$ versus *Run #* for Bi2212 tapes, where a "run" is defined as a heater pulse that may or may not induce a quench. If the heat pulse does not induce a quench, then the pulse amplitude is increased in the next

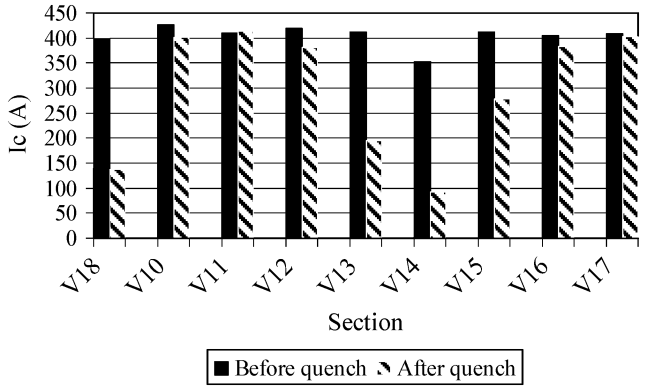


Fig. 22. Quench degradation in a Bi2212 round wire. Each section refers to a different location within one tape (V18 is end-to-end). With Bi2212 round wires, quench degradation is more difficult to induce than in Bi2212 tapes and is also more localized within the wire.

TABLE I
LIMITS TO AVOID QUENCH DEGRADATION IN BI2212 CONDUCTORS

| | Tape Conductor | Round Wire |
|---|---|---|
| $T_{peak}$ | < 300 K | < 330 K |
| $dT/dx$ | < 90 K/cm | < 100 K/cm |
| $dT/dt$ | < 150 K/s | < 250 K/s |

run. This process is repeated until a quench is obtained. This figure illustrates that no degradation occurs for heat pulses that do not result in a quench, but that every time a quench does result, the conductor performance is degraded. This was seen consistently for Bi2212 tapes. Fig. 22 shows results from a similar experiment on a Bi2212 round wire. In this case, it was found that the conductor could experience a quench and *not* necessarily experience degradation, as was the case with YBCO. By varying the length of the heater and the duration and amplitude of the heat pulses, the relative effects of the hot-spot temperature $(T_{peak})$, temperature gradient $(dT/dx)$ and rate of temperature change $(dT/dt)$ on the quench degradation were assessed and preliminary operational limits to prevent degradation were determined. These are summarized in Table I. While these values are considered preliminary, they illustrate that the Bi2212 round wires are more tolerant than the tape conductors. This is consistent with the higher $\varepsilon_c$ measured in Bi2212 round wires than in Bi2212 tape conductors.

## V. SUMMARY AND CONCLUSION

The development of high-field superconducting solenoids is being driven by the demands of scientific research. As $Nb_3Sn$ reaches its fundamental high-field limits, new conductor and magnet technologies are required. Emerging HTS conductors are poised to fill this need and their progress indicates the potential for generating magnetic fields significantly higher than previously envisioned. Large $J_c$(45 T) has been measured and insert coils above 25 T have been demonstrated.

At present it remains unclear which HTS conductor will emerge as the preferred option for high-field magnets. Just as high-field LTS magnets typically take advantage of both NbTi and $Nb_3Sn$, one can envision high-field HTS magnets with both YBCO and Bi2212 sections. YBCO has higher $J_c$, $J_E$ and mechanical strength, and is well understood. YBCO also has design flexibility in the selection of stabilizer, indicating that it may be possible to optimize the conductor mechanical and thermal behaviors for strength and quench protection, and in nanoinclusions for optimization of the electrical behavior for specific magnets. YBCO is limited, however, to wide tape geometries and at present has a fill factor $\sim$1%.

The implementation of Bi2212 poses many challenges due to high temperature heat treatment in oxygen and relatively poor strain tolerance. Bi2212 is available, however, as an isotropic round wire which may offer significant benefits and a 30–40% fill factor. Furthermore, there is no intrinsic reason that $J_c$ in YBCO should be significantly higher than in Bi2212. Thus, significant improvements in Bi2212 may be forthcoming as the research focus on this material increases. In comparing Bi2212 round wires and tapes, it is seen that the round wires have higher $J_c$, higher $J_E$, increased strain tolerance and improve quench tolerance. Although these are only a correlation at present, it is likely that these improvements are all the result of reduced filament size and improved microstructural characteristics. Thus, it is anticipated that as Bi2212 becomes better understood at the microstructural level, that all of these performance metrics will improve further.

In both YBCO and Bi2212 magnets, slow quench propagation velocity and high energy margin imply that HTS coils will be very stable and that quenching may be unlikely. The situation may be more complicated, however, in that the slow propagation does not necessarily imply that there is not a large hot-spot temperature, and a coil could be damaged without a traditional quench. It is interesting to note that the maximum hot-spot temperatures shown in Table I are higher than those typically allowed for LTS magnets. Thus, while the slow propagation may indicate that more time is available for active protection, it also implies that detection will be the most significant challenge [80]. Detection depends upon obtaining a measurable and distinguishable voltage over a significant length of conductor. Without propagation, a sufficient voltage may not be detected before damage is initiated. Note that voltage is a length-averaged quantity (more precisely, it is the integral of the electrical field over a length) and that two vastly different electric field profiles can result in the same end-to-end voltage. Conductor degradation, however, is the result of *local* conditions. Due to slow propagation, $T(x)$ and $V(x)$ in HTS coils are much more peaked than in LTS coils, so quench detection using a similar voltage criterion may result in damage to an HTS coil where it would not in an LTS coil. As a result, new approaches to quench detection may be required.

As HTS conductors continue to progress and the remaining problems solved, significant impact of these conductors on high-field magnets is anticipated in the years to come.

## ACKNOWLEDGMENT

The authors thank collaborators at American Superconductor Corporation, Oxford Superconducting Technology, Supercon, Inc. and SuperPower Inc. for use of conductors and for productive collaborations over the past ten years. The authors also thank David Larbalestier, Eric Hellstrom, Jianyi Jiang and W. Denis Markiewicz for many useful discussions.

## REFERENCES


[1] S. Ono, Y. Ando, F. F. Balakirev, J. B. Betts, and G. S. Boebinger, "Examination of the c-axis resistivity of $Bi_2Sr_{2-x}La_xCuO_{6+d}$ in magnetic fields up to 58 T," *Phys. Rev. B*, vol. 70, p. 224521, 2004.

[2] E. Y. Chekmenev, K. W. Waddell, J. Hu, Z. Gan, R. J. Wittebort, and T. A. Cross, "Ion binding study by $^{17}O$ solid-state NMR spectroscopy in a model peptide Gly-Gly-Gly at 19.6 T," *J. Am. Chem. Soc.*, vol. 128, pp. 9847–9855, 2006.

[3] D. Arcon, A. Zorko, M. Pregelj, J. Dolinsek, H. Berger, A. Ozarowski, H. van Tol, and L. C. Brunel, "High-field ESR in a two-dimensional $S = 1$ spin system $Ni_5(TeO_3)_4Br_2$," *J. Magn. Magn. Mater.*, vol. 316, no. 2, p. e349, 2007.

[4] H. Maeda, P. V. P. S. S. Sastry, U. P. Trociewitz, J. Schwartz, K. Ohya, M. Sato, W. P. Chen, K. Watanabe, and M. Motokawa, "Effect of magnetic field strength in melt-processing on texture development and critical current density of Bi-oxide superconductors," *Physica C Supercond.*, vol. 386, pp. 115–121, 2003.

[5] T. A. Houpt *et al.*, "Behavioral effects on rats of high strength magnetic fields generated by a resistive electromagnet," *Phys. and Behav.*, vol. 86, pp. 379–389, 2005.

[6] S. A. Gourlay, G. Sabbi, F. Kircher, N. Martovetsky, and D. Ketchen, "Superconducting magnets and their applications," *Proceedings of the IEEE*, vol. 92, no. 10, pp. 1675–1687, Oct. 2004.

[7] J. E. C. Williams, "Superconducting magnets and their applications," *Proceedings of the IEEE*, vol. 77, no. 8, pp. 1132–1142, Aug. 1989.

[8] R. M. Scanlan, A. P. Malozemoff, and D. C. Larbalestier, "Superconducting materials for large scale applications," *Proceedings of the IEEE*, vol. 92, no. 10, pp. 1639–1654, 2004.

[9] M. D. Bird, "Resistive magnet technology for hybrid inserts," *Supercond. Sci. Technol.*, vol. 17, pp. R19–R33, 2004.

[10] C. A. Swenson *et al.*, "Performance of 75 T prototype pulsed magnet," *IEEE Trans. Appl. Supercond.*, vol. 16, no. 2, pp. 1650–1655, June 2006.

[11] M. R. Vaghar, L. Li, Y. Eyssa, H. J. Schneider-Muntau, and R. Kratz, "Roads to 100 T pulsed magnets," *IEEE Trans. Appl. Supercond.*, vol. 10, no. 1, pp. 507–509, March 2000.

[12] J. R. Miller, "The NHMFL 45-T hybrid magnet system: Past, present, and future," *IEEE Trans. Appl. Supercond.*, vol. 13, no. 2, pp. 1385–1390, June 2003.

[13] W. D. Markiewicz *et al.*, "900 MHz wide bore NMR spectrometer magnet at NHMFL," *IEEE Trans. Appl. Supercond.*, vol. 10, no. 1, pp. 728–731, March 2000.

[14] T. H. Sefzik *et al.*, "Solid-state O-17 NMR in carbohydrates," *Chem. Phys. Lett.*, vol. 434, pp. 312–315, 2007.

[15] D. Luga, C. Morais, Z. Gan, D. Neuville, L. Cormier, and D. Massiot, "NMR heteronuclear correlation between quadrupolar nuclei in solids," *J. Am. Chem. Soc.*, vol. 127, p. 11540, 2005.

[16] A. Korepanova, J. D. Moore, H. B. Nguyen, Y. Hua, T. A. Cross, and F. Gao, "Expression of membrane proteins from Mycobacterium tuberculosis in Escherichia coli as fusions with maltose binding protein," *Protein Expression and Purification*, vol. 53, pp. 24–30, 2007.

[17] U.S. National Research Council's Committee on Opportunities in High Magnetic Field Science, Opportunities in High Magnetic Field Science National Academies Press. Washington, D.C., 2005.

[18] H. W. Weijers, U. P. Trociewitz, K. Marken, M. Meinesz, H. Miao, and J. Schwartz, "The generation of 25.05 T using a 5.11 T $Bi_2Sr_2CaCu_2O_x$ superconducting insert magnet," *Supercond. Sci. Technol.*, vol. 17, pp. 636–644, 2004.

[19] D. Hazelton, SuperPower Inc., Private Communication Aug. 2007.

[20] P. J. Lee, Applied Superconductiviity Center, National High Magnetic Field Laboratory, Florida State University [Online]. Available: http://www.magnet.fsu.edu/magnettechnology/research/asc/images/jcprog-06-112706col.png

[21] C. B. Eom *et al.*, "High critical current density and enhanced irreversibility field in superconducting $MgB_2$ thin films," *Nature*, vol. 411, pp. 558–560, 2001.

[22] V. Selvamanickam *et al.*, "Recent progress in second-generation HTS conductor scale-up at SuperPower," *IEEE Trans. Appl. Supercond.*, vol. 17, no. 2, pp. 3231–3234, June 2007.

[23] J. Jiang, Applied Superconductivity Center, National High Magnetic Field Laboratory, Florida State University, Private Communication 2007.

[24] K. R. Marken, Jr., H. P. Miao, M. Meinesz, B. Czabaj, and S. Hong, "Progress in Bi-2212 wires for high magnetic field applications," *IEEE Trans. Appl. Supercond.*, vol. 16, no. 2, pp. 992–995, June 2006.

[25] S. H. Wee, A. Goyal, J. Li, Y. L. Zuev, S. Cook, and L. Heatherly, "The incorporation of nanoscale columnar defects comprised of self-assembled BaZrO3 nanodots to improve the flux pinning and critical current density of NdBa2Cu3O7- $\delta$ films grown on RABiTS," *Supercond. Sci. Technol.*, vol. 20, no. 8, pp. 789–793, Aug. 2007.

[26] X. Y. Song *et al.*, "Evidence for strong flux pinning by small, dense nanoprecipitates in Sm-doped $YBa_2Cu_3O_{7-d}$ coated conductor," *Appl. Phys. Lett.*, vol. 88, no. 21, p. 212508, 2006.

[27] S. I. Kim *et al.*, "On the through-thickness critical current density of an $YBa_2Cu_3O_{7-x}$ film containing a high density of insulating, vortex-pinning nanoprecipitates," *Appl. Phys. Lett.*, vol. 90, p. 252502, 2007.

[28] M. W. Rupich *et al.*, "The development of second generation HTS wire at American Superconductor," *IEEE Trans. Appl. Supercond.*, vol. 17, no. 2, pp. 3379–3382, June 2007.

[29] H. Miao *et al.*, "High field insert coils from Bi-2212/Ag round wires," *IEEE Trans. Appl. Supercond.*, vol. 17, no. 2, p. 2262, 2007.

[30] T. M. Shen, X. T. Liu, U. P. Trociewitz, W. T. Nachtrab, T. Wong, and J. Schwartz, "Mechanical behavior of $Bi_2Sr_2CaCu_2O_x$ conductor using a split melt process for react-wind-sinter magnet fabrication," *IEEE Trans. Appl. Supercond.*, vol. 18, no. 2, June 2008.

[31] X. T. Liu, T. M. Shen, U. P. Trociewitz, and J. Schwartz, "React-wind-sinter processing of high superconductor fraction $Bi_2Sr_2CaCu_2O_x$/AgMg round wire," *IEEE Trans. Appl. Supercond.*, vol. 18, no. 2, June 2008.

[32] T. Koizumi *et al.*, "Bi-2212 phase formation process in multifilamentary Bi-2212/Ag wires and tapes," *IEEE Trans. Appl. Supercond.*, vol. 15, no. 2, pp. 2538–2541, 2005.

[33] H. Kitaguchi *et al.*, "Bi2Sr2CaCu2Ox/Ag multilayer tapes with Jc (4.2 K, 10 T) of 500,000 A/cm2 by using PAIR process," *IEEE Trans. Appl. Supercond.*, vol. 9, no. 2, pp. 1794–1799, 1999.

[34] T. Hasegawa *et al.*, "HTS conductors for magnets," *IEEE Trans. Appl. Supercond.*, vol. 12, no. 1, pp. 1136–1140, 2002.

[35] H. W. Weijers, J. Schwartz, B. ten Haken, M. Dhalle, and H. H. J. ten Kate, "Effects of conductor anisotropy on the design of Bi-Sr-Ca-Cu-O sections of 25 T solenoids," *Supercond. Sci. Technol.*, vol. 16, pp. 672–681, 2003.

[36] H. W. Weijers, B. ten Haken, H. H. J. ten Kate, and J. Schwartz, "Field dependence of the critical current and its relation to the anisotropy of BSCCO conductors and coils," *IEEE Trans. Appl. Supercond.*, vol. 15, no. 2, pp. 2558–2561, 2005.

[37] R. M. Scanlan *et al.*, "Fabrication and test results for Rutherford-type cables made from BSCCO strands," *IEEE Trans. Appl. Supercond.*, vol. 9, no. 2, pp. 130–133, 1999.

[38] D. R. Dietderich, E. Barzi, A. K. Ghosh, N. L. Liggins, and H. C. Higley, "Cable R&D for the LHC accelerator research program," *IEEE Trans. Appl. Supercond.*, vol. 17, no. 2, pp. 1481–1484, 2007.

[39] H. W. Weijers, J. M. Yoo, B. ten Haken, and J. Schwartz, "Bi-Sr-Ca-Cu-O conductors and magnets at high stress-strain levels," *Physica C Supercond.*, vol. 357–360, pp. 1160–1164, 2001.

[40] H. W. Weijers, J. Schwartz, and B. ten Haken, "Bi-based HTS insert coils at high stress levels," *Physica C Supercond.*, vol. 372–376, pp. 1364–1367, 2002.

[41] J. Kessler, S. Boutemy, S. Chen, D. Dimapilis, V. Miller, W. Wei, and J. Schwartz, "Preparation of dispersion-hardened single- and multifilamentary $Bi_2Sr_2CaCu_2O_x$ tapes and wires," *IEEE Trans. Appl. Supercond.*, vol. 7, no. 2, pp. 1560–1563, 1997.

[42] Q. Y. Hu, Y. Viouchkov, H. W. Weijers, and J. Schwartz, "Continuous processing of AgMg-sheathed $Bi_2Sr_2CaCu_2O_8$ tapes," *IEEE Trans. Appl. Supercond.*, vol. 9, no. 2, pp. 1808–1811, 1999.

[43] Q. Y. Hu, P. V. P. S. S. Sastry, U. P. Trociewitz, and J. Schwartz, "Microstructure and critical currents in AgMg-sheathed multifilamentary $Bi_2Sr_2CaCu_2O_8$ tapes," *IEEE Trans. Appl. Supercond.*, vol. 9, no. 2, pp. 1876–1879, 1999.

[44] H. W. Weijers *et al.*, "Development of 3 T class Bi-2212 insert coils for high field NMR," *IEEE Trans. Appl. Supercond.*, vol. 9, no. 2, pp. 563–566, 1999.

[45] H. W. Weijers *et al.*, "Development and testing of a 3 T Bi-2212 insert magnet," in *Adv. Cryogenic Engineering: Proc. Cryogenic Engr. Conf.*, 2000, vol. 45A, pp. 769–778.

[46] H. W. Weijers *et al.*, "Development of a 5 T HTS insert magnet as part of 25 T class magnets," *IEEE Trans. Appl. Supercond.*, vol. 13, no. 2, pp. 1396–1399, 2003.

[47] T. Hasegawa *et al.*, "Fabrication and properties of Bi2Sr2CaCu2Oy multilayer superconducting tapes and coils," *IEEE Trans. Appl. Supercond.*, vol. 7, no. 2, pp. 1703–1706, 1997.

[48] T. C. Holesinger *et al.*, "Isothermal melt processing of Bi-2212 tapes," *IEEE Trans. Appl. Supercond.*, vol. 9, no. 2, pp. 1800–1803, 1999.

[49] D. E. Wesolowski, M. O. Rikel, J. Jiang, S. Arsac, and E. E. Hellstrom, "Reactions between oxides and Ag-sheathed BiSrCaCuO conductor," *Supercond. Sci. Technol.*, vol. 18, pp. 934–943, 2005.

[50] U. P. Trociewitz, "Bi2212 conductor and coil technology for high field magnets," presented at the 20th International Conference on Magnet Technology, August 2007, unpublished.

[51] S. Boutemy, J. Kessler, and J. Schwartz, "React-wind-and-sinter technique for $Bi_2Sr_2CaCu_2O_8$ high $T_c$ coils," *IEEE Trans. Appl. Supercond.*, vol. 7, no. 2, pp. 1552–1555, 1997.

[52] J. Schwartz and G. A. Merritt, "Proof-of-principle experiments for react-wind-sinter manufacturing of $Bi_2Sr_2CaCu_2O_{8+x}$ magnets," *Supercond. Sci. Technol. Rapid Comm.*, vol. 20, pp. L59–L62, 2007.

[53] D. C. van der Laan, H. J. N. van Eck, B. ten Haken, H. H. J. ten Kate, and J. Schwartz, "Strain effects in high temperature superconductors investigated with magneto-optical imaging," *IEEE Trans. Appl. Supercond.*, vol. 13, no. 2, pp. 3534–3539, 2003.

[54] A. L. Mbaruku, I. Rutel, U. P. Trociewitz, H. W. Weijers, and J. Schwartz, "Electro-mechanical behavior of YBCO coated conductor in tension," in *Adv. Cryogenic Engineering: Proc. Int. Cryogenic Mater. Conf.*, 2004, vol. 50B, pp. 700–705.

[55] A. L. Mbaruku and J. Schwartz, "Fatigue behavior of Y-Ba-Cu-O coated conductor at 77 K," *IEEE Trans. Appl. Supercond.*, submitted for publication.

[56] D. C. van der Laan, J. W. Ekin, C. C. Clickner, and T. C. Stauffer, "Delamination strength of YBCO coated conductors under transverse tensile stress," *Supercond. Sci. Technol.*, vol. 20, no. 8, pp. 765–770, Aug. 2007.

[57] D. C. van der Laan and J. W. Ekin, "Large intrinsic effect of axial strain on the critical current of high-temperature superconductors for electric power applications," *Appl. Phys. Lett.*, vol. 90, p. 052506, 2006.

[58] N. Cheggour, J. W. Ekin, and C. L. H. Thieme, "Magnetic-field dependence of the reversible axial-strain effect in Y-Ba-Cu-O coated conductors," *IEEE Trans. Appl. Supercond.*, vol. 15, no. 2, pp. 3577–3580, 2005.

[59] J. Schwartz, B. C. Amm, H. Garmestani, D. K. Hilton, and Y. Hascicek, "Mechanical properties and strain effects in $Bi_2Sr_2CaCu_2O_x$/AgMg composite conductors," *IEEE Trans. Appl. Supercond.*, vol. 7, no. 2, pp. 2038–2041, 1997.

[60] Y. Viouchkov, H. W. Weijers, and J. Schwartz, "Stress-strain effects in Bi-2212 superconductors," *IEEE Trans. Appl. Supercond.*, vol. 10, no. 1, pp. 1134–1137, 2000.

[61] D. C. van der Laan, M. W. Davidson, B. ten Haken, H. H. J. ten Kate, and J. Schwartz, "Magneto-optical imaging study of the crack formation in superconducting tapes caused by applied strain," *Physica C Supercond.*, vol. 372–376, pp. 1020–1023, 2002.

[62] A. L. Mbaruku, K. R. Marken, M. Meinesz, H. Miao, P. V. P. S. S. Sastry, and J. Schwartz, "Effect of processing defects on stress-strain-$I_c$ for AgMg sheathed Bi-2212 tapes," *IEEE Trans. Appl. Supercond.*, vol. 13, no. 2, pp. 3522–3525, 2003.

[63] A. L. Mbaruku and J. Schwartz, "Statistical analysis of electro-mechanical properties of AgMg sheathed $Bi_2Sr_2CaCu_2O_{8+x}$ superconducting tapes using Weibull distributions," *J. Appl. Phys.*, vol. 101, no. 7, p. 073913, 2007.

[64] F. Trillaud, H. Palanki, U. P. Trociewitz, S. H. Thompson, H. W. Weijers, and J. Schwartz, "Normal zone propagation experiments on high temperature superconductor composite conductors," *Cryogenics*, vol. 43, no. 3–5, pp. 271–279, 2003.

[65] J. Lue *et al.*, "Quench tests of a 20-cm-long RABiTS YBCO tape," in *Adv. Cryogenic Engineering: Proc. Int. Cryogenic Mater. Conf.*, 2004, vol. 48, pp. 321–328.

[66] R. Duckworth *et al.*, "Quench dynamics in silver coated YBCO tapes," in *Adv. Cryogenic Engineering: Proc. Int. Cryogenic Mater. Conf.*, 2004, vol. 48, pp. 313–320.

[67] R. Grabovickic, J. W. Lue, M. Gouge, J. A. Demko, and R. Duckworth, "Measurements of temperature dependence of the stability and quench propagation of a 20-cm-long RABiTS Y-Ba-Cu-O tape," *IEEE Trans. Appl. Supercond.*, vol. 13, no. 2, pp. 1726–1730, 2003.

[68] R. Duckworth, J. W. Lue, D. Lee, R. Grabovickic, and M. Gouge, "The role of nickel substrates in the quench dynamics of silver coated YBCO tapes," *IEEE Trans. Appl. Supercond.*, vol. 13, no. 2, pp. 1768–1771, 2003.

[69] F. Trillaud, A. Caruso, J. Barrow, B. Trociewitz, U. P. Trociewitz, H. W. Weijers, and J. Schwartz, "Normal zone generation and propagation in $YBa_2Cu_3O_{7-\delta}$ coated conductors initialized by localized, pulsed disturbances," in *Adv. Cryogenic Engineering: Proc. Int. Cryogenic Mater. Conf.*, 2004, vol. 50B, pp. 852–859.

[70] X. R. Wang, A. R. Caruso, M. Breschi, G. M. Zhang, U. P. Trociewitz, H. W. Weijers, and J. Schwartz, "Normal zone initiation and propagation in Y-Ba-Cu-O coated conductors with Cu stabilizer," *IEEE Trans. Appl. Supercond.*, vol. 15, no. 2, pp. 2586–2589, 2005.

[71] M. Breschi, P. L. Ribani, X. Wang, and J. Schwartz, "Theoretical explanation of non-equipotential quench behavior in Y-Ba-Cu-O coated conductors," *Supercond. Sci. Technol. Rapid Comm.*, vol. 20, no. L9–L11, 2007.

[72] X. R. Wang, U. P. Trociewitz, and J. Schwartz, "Near adiabatic quench experiments on short $YBa_2Cu_3O_{7-\delta}$ coated conductors," *J. Appl. Phys.*, vol. 101, no. 5, p. 053904, 2007.

[73] G. A. Levin, P. N. Barnes, and J. S. Bulmer, "Current sharing between superconducting film and normal metal," *Supercond. Sci. Technol.*, vol. 20, no. 8, pp. 757–764, Aug. 2007.

[74] G. A. Levin and P. N. Barnes, "The normal zone in YBa2Cu3O6+x-coated conductors," *Supercond. Sci. Technol.*, vol. 20, no. 12, pp. 1101–1107, Dec. 2007.

[75] A. Ishiyama *et al.*, "Degradation of YBCO coated conductors due to over-current pulse," *IEEE Trans. Appl. Supercond.*, vol. 17, no. 2, pp. 3509–3512, June 2007.

[76] U. P. Trociewitz *et al.*, "Quench studies on a layer-wound $Bi_2Sr_2CaCu_2O_x$/AgX coil at 4.2 K," *Supercond. Sci. Technol.*, vol. 21, p. 025015, January 2008.

[77] T. Effio, U. P. Trociewitz, X. Wang, and J. Schwartz, "Quench induced degradation in $Bi_2Sr_2CaCu_2O_x$ at 4.2 K," *Supercond. Sci. Technol.*, to be published.

[78] T. Effio, U. P. Trociewitz, X. Wang, and J. Schwartz, "Quench induced degradation in $Bi_2Sr_2CaCu_2O_x$ round wires at 4.2 K," *Supercond. Sci. Technol.*, submitted for publication.

[79] T. Kiss *et al.*, "Quench characteristics in HTSC devices," *IEEE Trans. Appl. Supercond.*, vol. 9, no. 2, pp. 1073–1076, 1999.

[80] W. S. Kim, F. Trillaud, I. C. Ang, S. Y. Hahn, and Y. Iwasa, "Normal zone propagation in YBCO winding pack models," *IEEE Trans. Appl. Supercond.*, vol. 17, no. 2, pp. 2478–2481, 2007.

[81] F. Trillaud *et al.*, "Protection and Quench detection of YBCO coils results with small test coil assemblies," *IEEE Trans. Appl. Supercond.*, vol. 17, no. 2, pp. 2450–2453, 2007.

[82] A. L. Mbaruku, U. P. Trociewitz, X. R. Wang, and J. Schwartz, "Relationships between conductor damage, quenching and electromechanical behavior in YBCO coated conductors," *IEEE Trans. Appl. Supercond.*, vol. 17, no. 2, pp. 3044–3049, 2007.